Two-level Clustering-based Target Detection Through Sensor Deployment and Data Fusion

Chase Q. Wu, Wuji Liu
Dept of Computer Science
New Jersey Institute of Technology
Newark, NJ 07102
{chase.wu, wl87}@njit.edu

Satyabrata Sen, Nageswara S.V. Rao
Computational Sciences and Engineering Division
Oak Ridge National Laboratory
Oak Ridge, TN 37831
{sens, raons}@ornl.gov

Richard R. Brooks, Guthrie Cordone
Dept of Electrical and Computer Engineering
Clemson University
Clemson, SC 29634
{rrb, gcordon}@clemson.edu

***Abstract*—Target detection is one fundamental problem in many sensor network-based applications, and is typically tackled in two separate stages for sensor deployment and data fusion. We propose an integrated solution, referred to as SSEM, which combines 2-level clustering-based sensor deployment and Source Strength Estimate Map-based data fusion for the detection of a single static or moving target. SSEM conducts the first level of clustering to determine a sensor deployment scheme and the second level of clustering to divide the deployed sensors into multiple subsets. For each sensor, the source strength is estimated at each grid point of the entire region based on a signal attenuation model, and for each subset of sensors, the target location is estimated using a strength distribution map-based statistical analysis method. A final detection decision is made by thresholding the clustering degree of the target location estimates computed by all subsets of sensors. Compared with traditional grid-based target detection methods, SSEM significantly reduces the computation complexity and improves the detection performance through an integrated optimization strategy. Extensive simulation results show the performance superiority of the proposed solution over several well-known methods for target detection.**

***Index Terms*—Sensor networks; source detection; sensor deployment; cluster analysis.**

I. Introduction

Sensor networks have found pervasive applications in many agricultural, civil, industrial, and military domains for various purposes [1], [2], [3], [4], [5]. Target (or signal source) detection is considered as one of the fundamental problems in such sensor network-based applications and has been the focus of research for decades. Most of the existing research efforts on target detection are focused on one single technique through either data fusion or sensor deployment, and have met with considerable success in various contexts. However, combining multiple techniques from both aspects to improve runtime efficiency and detection performance still remains largely unexplored.

Several methods for target detection exemplified by Maximum Likelihood Estimation (MLE) [6] employ a grid-based data fusion approach. In such grid-based detection methods, the key idea is to construct a grid map of the entire region, use the signal probability density function to formulate a statistical framework at each grid point, and make a detection decision at the grid point with the highest probability. These traditional grid-based methods have won a good reputation with a satisfactory detection performance, but are generally computationally very expensive due to the complexity of the likelihood function, especially at high resolutions. More precisely, the detection performance of these methods highly depends on the accuracy of the likelihood function, which in turn determines the complexity of computation. There are cases where the likelihood function may be too complicated to calculate, e.g., in the radiation detection and localization problem with significant randomness in the source signal and background noise [7], [8]. In many cases for such problems, we may only be able to derive an approximate solution.

Sensor deployment has been another active research area for target detection (or region coverage) in many sensor network-based applications. Most of the conventional sensor deployment strategies consider two deployment objectives: i) minimize the deployment cost, which is generally determined by the number of sensors to be deployed in the region; and ii) maximize the detection performance such that the entire detection region is covered with the maximum signal strength [9], [10], [11].

In this paper, we propose an integrated solution, referred to as SSEM, to the detection of a single static or moving target through 2-level clustering-based sensor deployment and Source Strength Estimate Map-based data fusion. SSEM conducts the first level of clustering, where each grid point is a clustering object and each sensor is considered as a clustering center, to determine a sensor deployment scheme, and the second level of clustering to divide the deployed sensors into a number of subsets. For each sensor, the source signal strength is estimated at each grid point of the entire region based on a signal attenuation model, and for each subset of sensors, the target location is estimated using a distribution map-based statistical analysis method. A final detection decision is made by thresholding the clustering degree of the target location estimates computed by all subsets of sensors. Compared with traditional grid-based target detection methods, SSEM significantly reduces the computation complexity and improves the detection performance through an integrated optimization strategy. Extensive simulation results illustrate the performance superiority of the proposed integrated solution over several commonly used methods for target detection in practice.

The rest of this paper is organized as follows. Section II conducts a survey of related work. Section III formulates the target detection problem. Section IV proposes the SSEM detection method with the integration of sensor deployment and data fusion. Section V evaluates the performance of SSEM through simulations. Section VI concludes our work.

II. Related Work

A detection algorithm infers the presence or absence of a target or a signal source based on sensor measurements collected by a single or multiple sensors. In absence of noise and measurement errors, a detection can be made when the sensor receives a measurement that differs from the background profile. Unfortunately, in practice, sensor measurements are subject to statistical variations of the signal intensity and changes in the background noise.

Many methods and frameworks have been proposed and developed for target detection in different contexts, mainly in two categories: one is localization-based and the other is grid-based [6]. The methods in the first category include i) triangulation-based detection [12], [13], ii) Ratio of Squared Distance (RoSD)-based detection [14], and iii) time difference of arrival (TDoA)-based detection [15], [16], [17]. In general, these localization-based detection methods follow a similar 3-step procedure: a) use a certain signal attenuation model to build the relation between the source location and the signal strength; b) construct an equation system to solve for the source location; and c) use the estimated source location to make a detection decision. The main advantage of these methods is that there may exist a fast closed-form solution to the equation system, which makes it very efficient. However, if solving the equation system itself is prohibitively expensive or there are distractive solutions (e.g., "phantom" real roots or even imaginary roots) to the equation system, the robustness of a localization-based method would significantly decrease. The detection methods in the second category build a grid map of the entire region, use the signal probability density function to formulate a statistical framework at each grid point, and make a detection decision at the grid point with the maximum likelihood [18], [19], [20]. These methods are able to produce a robust and satisfactory detection performance but at the cost of expensive computation due to the complexity of the likelihood function or the high resolution of the grids.

Considering the pros and cons of the aforementioned traditional methods, this work combines a two-level clustering-based method for sensor deployment and a statistical analysis method with source location estimate distribution for data fusion to achieve a robust detection performance without involving complex optimization modeling or equation solving.

III. Problem Formulation

We consider the problem of deploying a given set of sensors in a two-dimensional (2D) continuous surveillance region R with an arbitrary shape to detect the existence of a potential static or moving target T. At each time step, a detection decision has to be made based on the sensor measurements.

This problem consists of two major components: sensor deployment that determines where to place sensors in the region and data fusion that determines how to integrate the measurements from individual sensors to make a global detection decision at each time step under two hypotheses: i) H_0: there is no target present, and ii) H_1: there is one target present. Under H_0, we wish to minimize the false alarm rate (FR), defined as the percentage of time steps that provide a false positive decision. Under H_1, we wish to minimize the missed detection rate (MR), defined as the percentage of time steps that provide a false negative decision.

In this typical passive target detection problem, we consider a generic signal attenuation model defined as a function f of the Euclidean distance d between each sensor and the target or source emitting the signal. The signal strength m emitted by a target T and received by the k-th sensor is calculated as

$$m_k = \frac{A}{f(d_k)} + B_k, \tag{1}$$

where A is the original signal strength of the target and B_k denotes the background noise observed by the k-th sensor under a certain probability distribution. Note that different targets (signal sources) such as radioactive, infrared, and acoustic sources feature different forms of signal attenuation. For example, in radiation detection, $f(\cdot)$ is typically modeled as a quadratic function. However, our proposed method is generic to tackle any form of $f(\cdot)$.

Obviously, on a 2D plane, there are at least two unknowns in Eq. 1, i.e., A and d_k (suppose that the background noise could be reasonably estimated from historical data). After replacing d_k and temporarily ignoring the background noise, we can rewrite Eq. 1 as

$$m_k = \frac{A}{f(\sqrt{(x_k - x_T)^2 + (y_k - y_T)^2})}, \tag{2}$$

where x_k and y_k are the coordinates of the k-th sensor, and x_T and y_T are the coordinates of the signal source or target T. If a sensor deployment scheme is given, we would know the location of each sensor. Hence, in Eq. 2, there are three unknowns, i.e., A, x_T, and y_T.

We formally define a passive target detection problem involving both sensor deployment and data fusion, referred to as PTD-SDDF, as follows.

Definition 1: PTD-SDDF: Given a set of n sensors $S = \{s_1, s_2, \ldots, s_n\}$, a potential target T of signal strength A with an attenuation model defined by Eq. 2, we wish to determine a sensor deployment scheme for the sensor set S and a data fusion scheme to integrate the measurement m_i from each individual sensor s_i, $i = 1, 2, \ldots, n$, at a certain time step such that the following detection performance is optimized:

$$\begin{cases} H_0 : \min(FR), \text{there is no target present,} \\ H_1 : \min(MR), \text{there is one target present.} \end{cases} \tag{3}$$

The difficulty of PTD-SDDF mainly arises from the fact that the source measurements under H_1 and the background noise under H_0 are comparable quantities and both contain significant random components in real environments especially outdoors, which rule out any deterministic optimal solution.

IV. Cluster-based Target Detection

We propose a two-level clustering-based solution using source strength estimate map, referred to as SSEM, which integrates sensor deployment and data fusion for the detection of a single static or moving target. We first present the overall structure of SSEM, and then details the rational behind the choice of methods for sensor deployment and data fusion.

A. Design of SSEM

The key steps of the proposed SSEM algorithm are provided in Alg. 1.

Algorithm 1 SSEM

Input: a set of n sensors s_i to be deployed in region R and the corresponding received signal strength m_i of each deployed sensor, $i = 1, 2, \ldots, n$.

Output: a sensor deployment scheme and a detection decision on the existence of a potential source.

1: Divide the region R into $p \times q$ uniform contiguous grids, each of which is indexed by a pair of (i, j), $i = 1, 2, \ldots, p$, $j = 1, 2, \ldots, q$.
2: Partition the grids into n clusters using the first-level k-means method and deploy one sensor at the center of each cluster.
3: Partition the deployed sensors into w non-overlapping subsets SS using the second-level k-means method.
4: At each time step, based on each sensor's measurement m_i, build a source strength estimate map by estimating the source strength at each grid according to the attenuation model.
5: For each subset SS of sensors, estimate the source location at the intersection grid of the source strength estimate maps produced by all sensors in the same subset.
6: Calculate the clustering degree or compactness of the source location estimates by all subsets of sensors obtained in Step 5.
7: Compare the clustering degree in Step 6 with a threshold: if the clustering degree is higher than the threshold, there is a source; otherwise, there is no source.

In Step 1, similar to many other grid-based detection approaches, the number of grids is determined by the requirements on the grid resolution and the constraint on the computational overhead.

In Step 2, we conduct the first-level clustering to decide a deployment scheme for the given sensors. In Step 3, we need to choose an appropriate value for the number w of subsets, which in turn determines the number of sensors in each subset. Having more sensors in the subset would gather more information about the source, but also increase the overhead of computation. In practice, we choose a value for w based on our empirical study such that the average number of sensors in each subset $\frac{n}{w} \geq 5$. When n is small, we may exhaust the combinations of w subsets to form $\sum_{i=1}^{n/w} C_{n/w}^{i}$ new subsets.

In Step 4, at each time step, based on the measurement of each deployed sensor, we build a source strength estimate map by estimating the source strength at each grid according to the signal attenuation model.

In Step 5, for each subset SS of sensors, we estimate the source location (x_T, y_T) to be the intersection grid of the source strength estimate maps produced by all sensors in the same subset, i.e., the grid (i, j) with the minimum variance of the source strength estimates, i.e.,

$$(x_T, y_T) = \underset{(x_i, y_j) \in R}{\operatorname{argmin}} \left(\frac{1}{|SS|} \cdot \sum_{\forall s_l \in SS} (\hat{A}_l - \bar{A})^2 \right), \quad (4)$$

where (x_i, y_j) are the coordinates of each grid (i, j) within region R, $\hat{A}_l$ is obtained in Step 4, i.e., the estimated signal strength calculated by Eq. 2 with the measurement m_l of sensor s_l in the sensor subset under the assumption that the source is located within the current grid (i, j), and $\bar{A}$ is the average signal strength estimate at (i, j) over the sensor subset.

In Step 6, there are different ways to calculate the clustering degree for measuring the compactness of all source estimates obtained in Step 5 [21], [22]. In this work, the clustering degree is reflected by the sum of the distances between the source estimates and their centroid. A higher clustering degree means a more dense (or compact) distribution of the calculated source estimates.

We would like to point out that SSEM does not involve any complex optimization model. The time complexity of SSEM is $O(p \cdot q \cdot n + w)$, where w is the number of sensor subsets, excluding the standard k-means method in Steps 2 and 3, which can be done offline. Moreover, since the signal strength estimation at each grid for each sensor is independent of each other, the algorithm framework of SSEM can be parallelized for higher runtime efficiency.

B. Sensor Deployment for Target Detection

Sensor deployment is an important component of SSEM. We employ a clustering-based sensor deployment strategy with the following considerations:

i) If there is no source, the deployment scheme should lead to a low clustering degree of the estimated source locations computed by all subsets of sensors; otherwise, it should lead to a high clustering degree. If the sensors are deployed too close to each other, they would produce similar measurements regardless of the existence of a source. In this case, no matter how subsets are divided, the source locations estimated by all sensor subsets would be close to each other, leading to a high clustering degree and hence making it hard to determine whether or not there is a true source.

ii) The received signal strength of each sensor should be high enough to resist the background noise at each possible source location. Since the received signal strength depends on the distance between the sensor and the source, each possible source location, i.e., each grid point, should be close enough to some sensors to produce a high received signal strength.

The above two considerations are aligned well with those in a typical clustering problem: i) within each cluster, the objects should be as close to the corresponding cluster center as possible; while ii) the distance between two cluster centers should be as far as possible. Therefore, we model the sensor deployment problem as a clustering problem, where the number of clusters is the number of sensors to be deployed. There exist many algorithms for this type of semi-supervised clustering problem, including the k-means method. By applying the k-means clustering model to our sensor deployment problem, we have the following optimization objective:

$$\min \sum_{i=1}^{n} \sum_{(p_j, q_j) \in C_i} w_j \cdot (\|p_j - u_i\|^2 + \|q_j - v_i\|^2), \quad (5)$$

where p_j and q_j denote the location of the j-th grid point, u_i and v_i denote the location of the i-th sensor, k is the

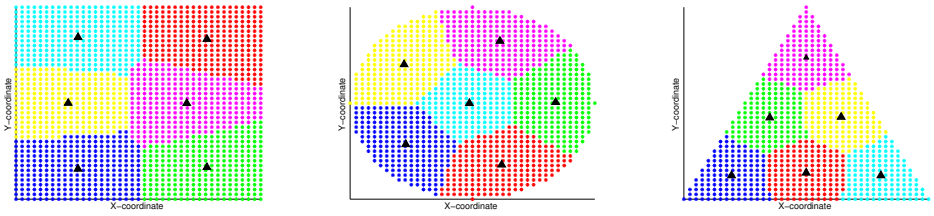

(a) (b) (c)

Fig. 1. Deployment of six sensors using the k-means method in (a) a square region, (b) a circular region, and (c) a triangular region.

number of sensors and C_i denotes the i-th cluster. The weight coefficient w_i could be used to assign a priority to certain areas. For illustration purposes, Fig. 1 plots several simple and representative deployment schemes for a given set of six sensors, obtained by the k-means method, in which the weight coefficient w_i's are set to be 1. In addition, different colors represent different clustering results and the black triangular marks correspond to the sensor locations. Fig. 1(a)(b)(c) plot the sensor deployment scheme for target detection in a square, circular, and triangular region, respectively.

C. Grid-based Data Fusion

In SSEM, the region R is first divided into a number of uniform contiguous grids, each of which is indexed by a pair of (i, j). Assuming that a source be located at a certain grid point, for a given sensor deployment scheme, we can estimate the signal strength A based on the measurement of each deployed sensor under a given attenuation model according to Eq. 2. Obviously, the accuracy of the signal strength estimate depends on the distance between the grid point where the source is assumed to exist and the true location of the source: the closer this grid point is to the true source location, the higher accuracy the source signal strength estimate has. Hence, the grid point that is the closest to the true source location would lead to the most accurate estimates of the true signal strength. The similarity of such signal strength estimates could be measured by their variance and used to derive the existence of a target.

However, even if there is no source present, there still exists a grid point with the minimum variance of the signal strength estimates. To resolve this issue, we partition the deployed sensors into a number of subsets and use each subset of sensors to find the source location with the minimum variance of the signal strength estimates. If there is a source present, each subset of sensors would lead to a similar source location estimate; otherwise, each subset of sensors would lead to a different source location estimate. Therefore, we may make a detection decision based on the clustering degree of the source location estimates calculated from all subsets of sensors.

V. Performance Evaluation

We conduct a simulation-based performance evaluation and illustration of the proposed SSEM method in comparison with several existing methods for passive target detection widely adopted in real applications. We shall start with a brief introduction to the methods in comparison.

A. Detection Methods in Comparison

1) Sequential Probability Ratio Test (SPRT)

SPRT is a classical target detection method that makes a detection decision under two hypotheses (a null hypothesis H_0 and an alternate hypothesis H_1) or rejects to make a decision [23]. SPRT accumulates the measurements m from n sensors within a time window of t time steps, denoted by $M = \{m_i^k\}$, $i = 1, 2, \cdots, n$, and $k = 1, 2, \ldots, t$, and defines a lower threshold $TH(H_0)$ and an upper threshold $TH(H_1)$. It then calculates a probability ratio $L = \frac{P(M|H_1)}{P(M|H_0)}$ and compares it with these two thresholds: if L is below $TH(H_0)$ or above $TH(H_1)$, it claims no source present or the presence of a source; otherwise, it rejects to make a decision. It is worth pointing out that SPRT has four parameters to be set, i.e., the required false alarm rate, the required missed detection rate, and the received signal strength and the background noise for each sensor. However, it is generally difficult to set these parameter values, especially the signal strength. In our experiments, we choose appropriate values for these parameters based on the models used to generate the measurement data.

2) Majority Vote (MV)

MV is a simple hard fusion method for target detection, whose key idea is as follows: each sensor makes a local binary detection decision based on its received signal strength and a predefined threshold, and a global decision is reached based on the rule of "majority wins". There is no systematic guideline on setting an appropriate threshold for MV. In our experiments, we set it to be the mean of the background noise to minimize the missed detection rate.

B. Experiment Set 1 on Manually Generated Data

1) Simulation Settings

In the first set of simulations, we consider a square region of $10m \times 10m$, which is divided into a set of grids with an interval of 0.1 meters along both dimensions. We consider 7 problem sizes based on 15 to 45 sensors with an increment of 5 sensors, available for deployment within the given region.

We run the detection experiments in two cases:

- Case 1: a single static source with weak or strong signal strength;
- Case 2: a single moving source with weak or strong signal strength.

In Case 1, the experiment lasts for 2 minutes: in the first 60 seconds, there is no source present, and in the last 60 seconds, there exists a static source. In Case 2, the experiment lasts for

40 seconds: in the first 20 seconds, there is no source present, and in the last 20 seconds, there exists a moving source. Under each case, we repeat the experiments 10 times with different random seeds and measure the average detection performance.

In the simulation, we manually generate the source signal strength A and the background noise b_k for sensor s_k, both following the Poisson distribution, and adopt a quadratic signal attenuation model:

$$m_k = \frac{A}{d_k^2} + b_k, \tag{6}$$

which represents a typical scenario in radiation detection [19], [24], [25], [26].

In all these experiments, the average strength of the background noise, i.e., the mean value of the Poisson distribution, is set to be 200 counts per second. The weak signal strength is set to be 400 counts per second, and the strong one is set to be 2000 counts per second. In Case 1, we randomly place a static source inside an area of $5m \times 5m$ at the center of the region. In Case 2, we simulate a target with either weak or strong signal moving from position (30, 30) to position (-30, -30) across the region at the speed of $(-0.1, -0.1)m/s$. SPRT and MV are executed for detection based on the sensor deployment scheme determined by SSEM.

2) Comparison of Detection Performance

We tabulate the average detection performance in terms of false alarm rate (FR) and missed detection rate (MR) for MV, SPRT and SSEM in Table I. Since MV compares the current measurement with the mean of the background noise, it exhibits a high detection rate (0% missed detection rate) in the presence of a static or moving target. However, this method is not practically useful as it is very sensitive with a false alarm rate of about 50%. Similarly, in SPRT, we adopt the parameters for simulation data generation, and it performs very well when there is no target present (0% false alarm rate). However, since SPRT attempts to accumulate the measurements over time, there is a delay effect in the detection of a source, hence resulting in a high missed detection rate. In general, it is challenging to set suitable parameter values in SPRT, which limits its practical use. Compared with these two traditional methods, the proposed SSEM method achieves a reasonable detection performance in terms of both FR and MR.

3) Illustration of Algorithm Execution

In order to examine the microscopic behaviors of the detection methods in comparison, we provide a detailed illustration of each algorithm execution with 20 sensors.

a) Case 1: A Single Static Target with Weak or Strong Signal

We plot the sensor deployment scheme in Fig. 2 and partition the sensors into $w = 4$ subsets using the k-means method. Since the number of subsets is limited, we exhaust the combinations of these 4 subsets to generate more (partially overlapping) subsets to calculate the clustering degree.

The experimental results in the static case are shown in Fig. 3. The detection results obtained by MV with weak and strong signal are plotted in Fig. 3(a) and Fig. 3(b), respectively, where the value of '1' means that there is a source and the value of '-1' means that there is no source (the same below).

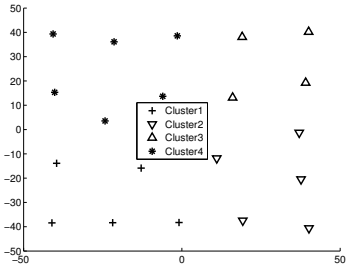

Fig. 2. The deployment of 20 sensors partitioned into 4 subsets in unit of decimeter.

In these two experiments, the threshold of each sensor is set to be the average background noise strength, i.e., 200 counts per second. In Fig. 3(a) and Fig. 3(b), we observe that MV has an FR of 56.67% and 46.67%, respectively, in the first 60 seconds, and exhibits a good detection performance with an MR of 0% in the last 60 seconds.

The results obtained by SPRT with weak and strong signal strengths are plotted in Fig. 3(c) and Fig. 3(d), respectively. SPRT has the following parameters: a required false alarm rate of 5%; a required missed detection rate of 5%; a background noise strength of 150 counts per second with weak signal and of 250 counts per second with strong signal; a received signal strength of 250 counts per second with weak signal and of 550 counts per second with strong signal. For an effective comparison, we choose suitable values for these parameters based on the models used in the simulation. In Fig. 3(c) and Fig. 3(d), we observe that SPRT exhibits a good performance with an FR of 0% in the first 60 seconds. Due to the delay effect caused by the accumulation of measurements over time, it does not perform well in the first half period of the last 60 seconds, resulting in an MR of 51.67% and 20%, respectively.

The clustering degree of source location estimates in SSEM is represented by the average distance between the source location estimates and their center. The detection patterns with weak and strong signal strengths are plotted in Fig. 3(e) and Fig. 3(f), respectively, in which, the horizontal line with the value of 77 (the same below) represents the threshold of the average distance: if the average distance is higher than the threshold line, claim no source; otherwise, claim a source. In Fig. 3(e), we observe that when the signal strength is weak, SSEM still exhibits a good performance with an FR of 5% and an MR of 3.3%. In Fig. 3(f), we observe that with strong signal strength, the detection pattern is much clearer, resulting in an FR of 6.67% and an MR of 0%.

The results in Fig. 3 show that in the static case, SSEM exhibits an overall superior performance over MV and SPRT.

b) Case 2: A Single Moving Target with Weak or Strong Signal

Fig. 4. shows the experimental results of the moving case. The results obtained by MV with weak and strong signal strengths are plotted in Fig. 4(a) and Fig. 4(b), respectively. In these two experiments, the threshold of each sensor is also set to be the average background noise, i.e., 200 counts per

TABLE I
COMPARISON OF DETECTION PERFORMANCE OF MV, SPRT, AND SSEM USING MANUALLY GENERATED DATA.

Prob Size (Number of Sensors)	MV (%)				SPRT (%)				SSEM (%)			
	Static Source		Moving Source		Static Source		Moving Source		Static Source		Moving Source	
	FR	MR	FR	MR	FR	MR	FR	MR	FR	MR	FR	MR
15	50.00	0	54.00	0	0	63.00	0	72.00	3.67	9.00	1.50	38.00
20	47.67	0	44.00	0	0	56.00	0	79.00	8.30	0.67	5.50	20.00
25	45.67	0	59.50	0	0	37.33	0	75.50	8.00	1.30	5.50	22.50
30	46.00	0	50.00	0	0	46.33	0	71.50	5.00	2.30	8.00	18.00
35	58.67	0	54.00	0	0	48.67	0	74.00	0	6.70	8.50	23.00
40	48.00	0	51.50	0	0	38.67	0	70.00	2.50	0	2.50	23.50
45	56.00	0	54.00	0	0	34.33	0	75.00	0.60	1.67	9.50	19.50

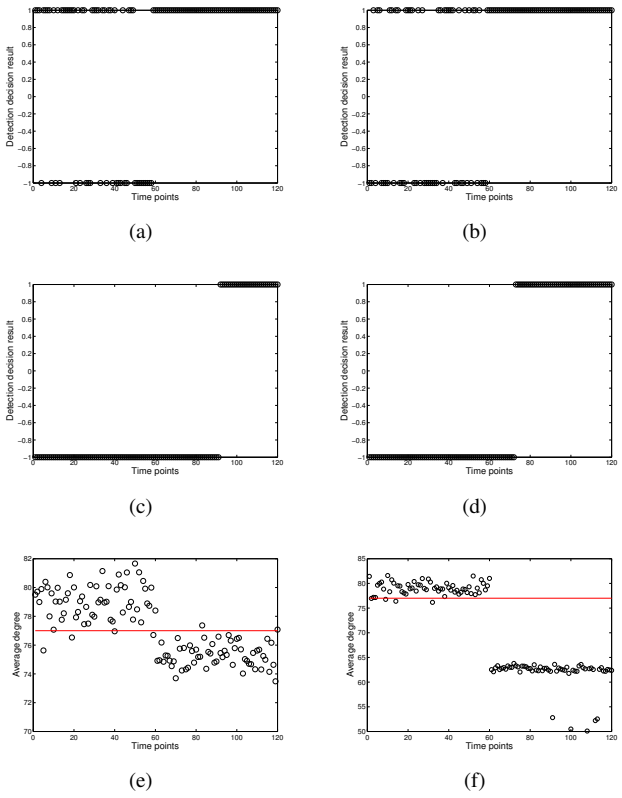

(a) (b) (c) (d) (e) (f)

Fig. 3. The detection results in the static case: (a) MV with weak signal strength, (b) MV with strong signal strength, (c) SPRT with weak signal strength, (d) SPRT with strong signal strength, and the detection patterns of (e) SSEM with weak signal strength, and (f) SSEM with strong signal strength.

second. We observe that the performance of MV in the moving case is similar to that in the static case with an FR of 45%.

The detection results of SPRT with weak and strong signal strengths in the moving case are plotted in Fig. 4(c) and Fig. 4(d), respectively. We choose the values for the four parameters of SPRT as follows: a required false alarm rate of 5%, a required missed detection rate of 5%, a background noise strength of 180 counts per second with weak signal and 200 counts per second with strong signal, and a received signal strength of 400 counts per second with weak signal and 2000 counts per second with strong signal. In these experiments, we observe that SPRT achieves a good detection performance as in the static case when there is no source present, but has a missed detection rate of 60% and 50% with weak and strong signal strength, respectively, in the presence of a moving source.

The detection patterns (i.e., the average distance between the source estimates and their center) in SSEM with weak and strong signal strengths are plotted in Fig. 4(e) and Fig. 4(f), respectively. The threshold of the average distance is again set to be 77 using the same subsets of sensors as in the static case. In Fig. 4(e), we observe that SSEM achieves a false alarm rate of 20% and a missed detection rate of 15% with a weak signal strength. In Fig. 4(f), we observe that the detection pattern is much clearer with strong signal strength, resulting in a false alarm rate of 0% and a missed detection rate of 20%. It is worth pointing out that the detection pattern in the moving case in the presence of a source exhibits a quadratic curve, whose lowest point corresponds to the moment when the source is approaching the center of the detection region such that every sensor is receiving a certain amount of signal. As the source is moving away from the center of the detection region, the sensors receive a smaller amount of signal, hence leading to a larger average distance or a lower degree of clustering.

The above results show that SSEM exhibits an overall superior performance over MV and SPRT in the moving case.

4) Illustration of SSEM under Different Resolutions

The performance of SSEM depends on the grid resolution. Fig. 5 shows the clustering pattern of the source estimates for target detection in SSEM under different resolutions. Fig. 5(a)(c)(e) plot the degree of clustering in the static case under the resolutions of 1m, 0.5m, and 0.2m, respectively, and Fig. 5(b)(d)(f) plot the degree of clustering in the moving case under the resolutions of 1m, 0.5m, and 0.2m, respectively. The detection pattern becomes clearer as the resolution increases.

C. Experiment Set 2 on Synthetic Radiation Data

1) Simulation Settings

We run the second set of experiments on synthetic radiation data generated by the method in [27] in the same square region of $10m \times 10m$, divided into 100×100 grids with an interval of 0.1 meters along both dimensions. The average background noise is set to be 250 counts per second. Similar to the static case in Experiment Set 1 on manually generated data, each experiment lasts for two minutes: no source during the first minute and a radiation source with a strength of 500 counts per second is placed at the center grid (50, 50) during the second minute. Again, the number of sensors is increased from 15 to 45 with an interval of 5 sensors, and in each run of SSEM,

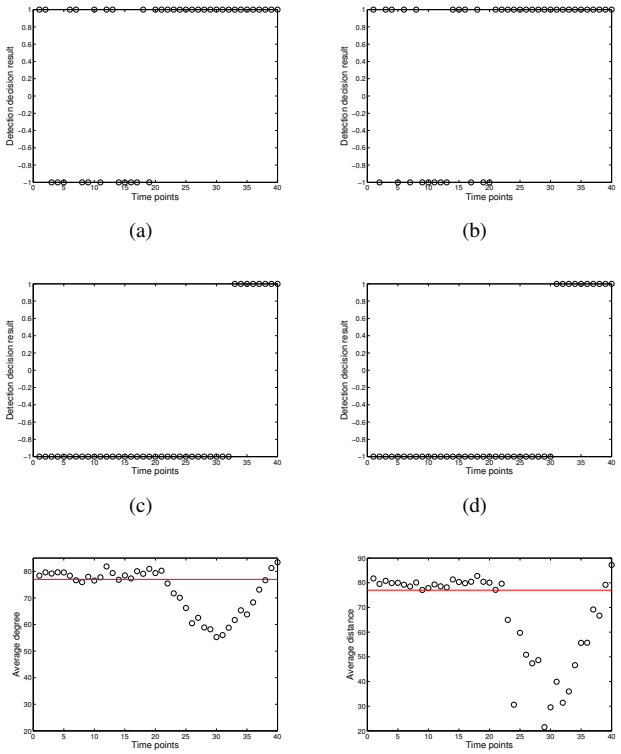

Fig. 4. The detection results in the moving case: (a) MV with weak signal strength, (b) MV with strong signal strength, (c) SPRT with weak signal strength, (d) SPRT with strong signal strength, and the detection patterns of (e) SSEM with weak signal strength, and (f) SSEM with strong signal strength.

TABLE II
COMPARISON OF DETECTION PERFORMANCE OF SPRT AND SSEM USING SYNTHETIC DATASETS.

Number of Sensors	SPRT (%)		SSEM (%)	
	FR	MR	FR	MR
15	0	17.39	5.88	7.56
20	0	21.70	6.72	4.20
25	0	11.30	7.56	1.68
30	0	9.56	5.88	2.52
35	0	7.80	3.36	3.36
40	0	10.40	4.20	2.52
45	0	6.95	3.30	0.84

these sensors are partitioned into 5 subsets. The parameter values of SPRT remain the same as those in Experiment Set 1.

2) Performance Comparison

The performance comparison in terms of both FR and MR between SPRT and SSEM is tabulated in Table II. The MV method is not included for comparison in these experiments as it tends to yield a high FR if the threshold is set to be the mean of background noise as in the first set of experiments, and also a high MR when the majority of the sensors fail to detect the source when they are far away from it with an increased threshold. We observe that SPRT still performs well in terms of FR but yields a high MR as in Experiment Set 1. These results show that SSEM exhibits an overall superior detection performance on the synthetic radiation datasets.

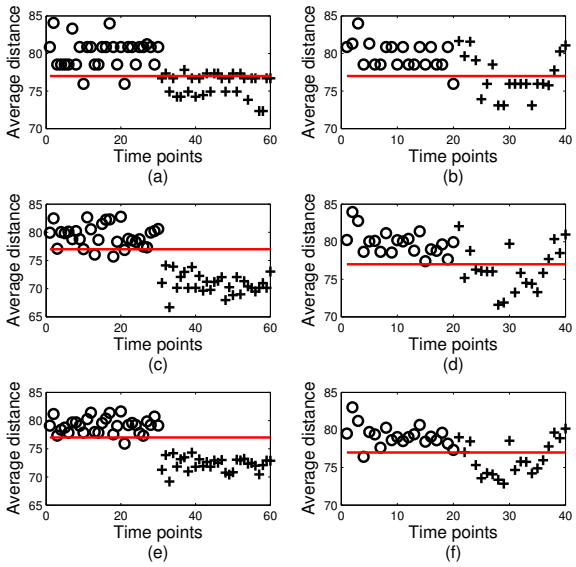

Fig. 5. The detection patterns in SSEM under different grid resolutions: the circles represent the situations without a source, and the pluses represent the situations with a static or moving source.

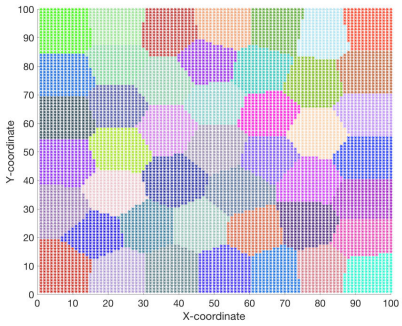

Fig. 6. Grid partitions for the deployment of 45 detectors after the first-level k-means clustering.

3) Illustration of SSEM

Fig. 6 shows the region partitioning for the deployment of 45 sensors produced by the first-level k-means clustering. These sensors are almost evenly distributed across the entire region. Fig. 7 shows the distribution maps of source strength estimates calculated based on the measurements of three sensors. We observe that these three distribution maps create a small intersection area, and the grid within this intersection area corresponding to the source location has the minimum variance of source strength estimates. Fig. 8 plots the variation of clustering degrees in SSEM with no source in the first 60 seconds and with a source in the last 60 seconds. Obviously, we are able to place a threshold line to separate these two scenarios for target detection.

VI. CONCLUSION

Target detection is one fundamental problem in many sensor network-based applications. We proposed an integrated

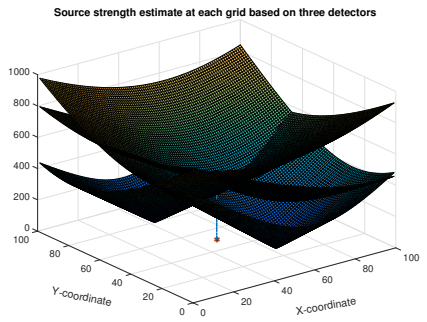

Fig. 7. The distribution of source strength estimates calculated based on each sensor (three sensors are used for illustration).

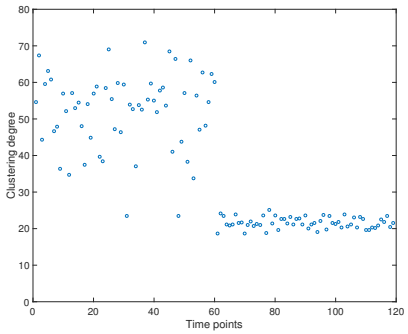

Fig. 8. The variation of clustering degrees in SSEM with no source in the first 60 seconds and with a source in the last 60 seconds.

method that combines both sensor deployment and data fusion for the detection of a single static or moving target. Extensive experimental results show that, under the considered scenarios, the proposed solution is more effective than several well-known methods for target detection in a static or moving case.

Similar to other threshold-based detection methods, the threshold used in SSEM has a critical impact on the detection performance. Instead of deriving a threshold based on the footprint of the sensor deployment, it is of our interest to develop a systematic approach to decide the threshold. Also, we will compare the time complexity with other grid-based detection methods and determine an appropriate resolution to meet the time requirement of the application.

ACKNOWLEDGMENTS

This work has been supported by the U.S. Department of Homeland Security, Domestic Nuclear Detection Office, under competitively awarded contract No. IAA HSHQDC-13-X-B0002. This support does not constitute an express or implied endorsement on the part of the Government.

REFERENCES

[1] A. Hyder, E. Shahbazian, and E. Waltz. *Multisensor Fusion*. Kluwer Academic, Boston, Mass, USA, 2002.

[2] I.F. Akyildiz, W. Su, Y. Sankarasubramaniam, and E. Cayirci. Wireless sensor networks: A survey. *COMNET*, 38(4):393–422, 2002.

[3] D. Culler, D. Estrin, and M. Srivastava. Overview of sensor networks. *IEEE Computer*, 37:41–49, Aug 2004.

[4] P.K. Varshney. *Distributed Detection and Data Fusion*. Springer-Verlag, New York, 1996.

[5] K. Chakrabarty, S.S. Iyengar, H. Qi, and E. Cho. Grid coverage for surveillance and target location in dsns. *IEEE Transactions on Computers*, 51(12):1448–1453, 2002.

[6] Y. Cheng and T. Singh. Source term estimation using convex optimization. In *Proc. of the 11th Int. Conf. on Information Fusion*, pages 1–8, Jun 2008.

[7] G. F. Knoll. *Radiation Detection and Measurement*. John Wiley, 2000.

[8] D. Mihalas and B. W. Mihalas. *Foundations of Radiation Hydrodynamics*. Courier Dover Publications, 2000.

[9] W. Shen and Q. Wu. Exploring redundancy in sensor deployment to maximize network lifetime and coverage. In *8th Annual IEEE Communications Society Conference on Sensor, Mesh and Ad Hoc Communications and Networks*, pages 557–565, Jun 2011.

[10] Y. Gu, Q. Wu, and N.S.V. Rao. Optimizing cluster heads for energy efficiency in large-scale heterogeneouswireless sensor networks. *Int. Journal of Distributed Sensor Networks*, 2010:1–9, Dec 2010.

[11] Q. Wu, N.S.V. Rao, X. Du, S.S. Iyengar, and V.K. Vaishnavi. On efficient deployment of sensors on planar grid. *Computer Communications Special Issue (SI) on Network Coverage and Routing Schemes for Wireless Sensor Networks*, 30(14-15):2721–2734, October 2007.

[12] N.S.V. Rao, M. Shankar, J.-C. Chin, D.K.Y. Yau, S. Srivathsan, S.S. Iyengar, Y. Yang, and J.C. Hou. Identification of low-level point radiation sources using a sensor network. In *Int. Conf. on Information Processing in Sensor Networks*, pages 493–504, Apr 2008.

[13] N.S.V. Rao, X. Xu, and S. Sahni. A computational geometric method for dtoa triangulation. In *Int. Conf. on Information Fusion*, pages 1–7, July 2007.

[14] J.-C. Chin, D.K.Y. Yau, N.S.V. Rao, C.Y.T. Ma, and M. Shankar. Accurate localization of low-level radioactive source under noise and measurement errors. In *Proc. of the 6th ACM conference on Embedded network sensor system*, pages 183–196, Jun 2008.

[15] X. Cheng, A. Thaeler, G. Xue, and D. Chen. Tps: A time-based positioning scheme for outdoor wireless sensor networks. In *Proc. of the 23rd IEEE INFOCOM*, pages 2685–2696, Hong Kong, China, March 2004.

[16] G. Mellen II, M. Pachter, and J. Raquet. Closed-form solution for determining emitter location using time difference of arrival measurements. *IEEE Trans. Aerospace and Electronic Systems*, 39(3):10561058, July 2003.

[17] A. Thaeler, M. Ding, and X. Cheng. itps: An improved location discovery scheme for sensor networks with long-range beacons. *JPDC*, 65(2):98–106, 2005.

[18] X. Sheng and Y.-H. Hu. Maximum likelihood multiple-source localization using acoustic energy measurements with wireless sensor networks. *IEEE Trans. on Signal Processing*, 53(1):44–53, Jan 2005.

[19] M. Morelande, B. Ristic, and A. Gunatilaka. Detection and parameter estimation of multiple radioactive sources. In *Proc. of the IEEE 10th Int. Conf. on Information Fusion*, pages 1–7, 2007.

[20] J.C. Chen, R.E. Hudson, and K. Yao. Maximum-likelihood source localization and unknown sensor location estimation for wideband signals in the near-field. *IEEE Trans. on Signal Processing*, 50(8):1843–1854, Aug 2002.

[21] R.O. Duda, D.G. Stork, and P.E. Hart. *Pattern Classification*. Wiley-Interscience, 2000.

[22] J. Han and M. Kamber. *Data Mining: Concepts and Techniques*. Elsevier(Singapore)Pte Ltd, 2nd edition, 2008.

[23] K.D. Jarman, L.E. Smith, and D.K. Carlson. Sequential probability ratio test for long-term radiation monitoring. *IEEE Trans. on Nuclear Science*, 51(4):1662–1666, Aug 2004.

[24] S. Brennan, A. Mielke, and D. Torney. Radioactive source detection by sensor networks. *IEEE Trans. on Nuclear Science*, 52(3):813–819, 2005.

[25] M. Morelande and B. Ristic. Radiological source detection and localisation using bayesian techniques. *IEEE Trans. on Signal Processing*, 57(11):4220–4231, 2009.

[26] B. Ristic, M. Morelande, and A. Gunatilaka. Information driven search for point sources of gamma radiation. *ACM Signal Processing*, 90(4):1225–1239, 2010.

[27] S. Sen, N.S.V. Rao, G. Cordone, R.R. Brooks, C.Q. Wu, M.L. Berry, and K.M. Grieme. Synthesis of radiation counts for networks of detectors. In *Proc. of Nuclear Science Symposium*, Atlanta, Georgia, USA, October 21-28 2017.